Published in final edited form as:

Cell Rep. 2018 May 08; 23(6): 1620–1629. doi:10.1016/j.celrep.2018.03.123.

Self-Condensation Culture Enables Vascularization of Tissue Fragments for Efficient Therapeutic Transplantation

Yoshinobu Takahashi[1], **Keisuke Sekine**[1], **Tatsuya Kin**[2], **Takanori Takebe**[1,3,4,5,6,7,*], **Hideki Taniguchi**[1,3,*]

[1]Department of Regenerative Medicine, Yokohama City University Graduate School of Medicine, Kanazawa-ku 3-9, Yokohama, Kanagawa 236-0004, Japan

[2]Clinical Islet Laboratory, University of Alberta, Edmonton, AB, Canada

[3]Advanced Medical Research Center, Yokohama City University, Kanazawa-ku 3-9, Yokohama, Kanagawa 236-0004, Japan

[4]Division of Gastroenterology, Hepatology & Nutrition, Developmental Biology, Center for Stem Cell and Organoid Medicine (CuSTOM), Cincinnati Children's Hospital Medical Center, 3333 Burnet Avenue, Cincinnati, OH 45229-3039, USA

[5]Department of Pediatrics, University of Cincinnati College of Medicine, 3333 Burnet Avenue, Cincinnati, OH 45229-3039, USA

[6]Institute of Research, Tokyo Medical and Dental University, 1-5-45 Yushima, Bunkyo-ku, Tokyo 113-8510, Japan

[7]Lead Contact

SUMMARY

Clinical transplantation of tissue fragments, including islets, faces a critical challenge because of a lack of effective strategies that ensure efficient engraftment through the timely integration of vascular networks. We recently developed a complex organoid engineering method by "self-condensation" culture based on mesenchymal cell-dependent contraction, thereby enabling dissociated heterotypic lineages including endothelial cells to self-organize in a spatiotemporal manner. Here, we report the successful adaptation of this method for generating complex tissues from diverse tissue fragments derived from various organs, including pancreatic islets. The self-condensation of human and mouse islets with endothelial cells not only promoted functionalization in culture but also massively improved post-transplant engraftment.

*Correspondence: takanori.takebe@cchmc.org (T.T.), rtanigu@yokohama-cu.ac.jp (H.T.).

AUTHOR CONTRIBUTIONS

Y.T. acquired, analyzed, and interpreted the data and wrote the manuscript. T.T. acquired, analyzed, and interpreted the data; wrote the manuscript; obtained funding; and supervised the study. T.K. isolated and provided the human islets. K.S. and H.T. supervised the study.

DECLARATION OF INTERESTS

T.T. and H.T. have served on scientific advisory boards for Healios Inc. T.T., Y.T., and H.T. have also granted a license to Healios through Yokohama City University over their inventions that relate to the subject of this manuscript.

SUPPLEMENTAL INFORMATION

Supplemental Information includes three figures and two videos and can be found with this article online at https://doi.org/10.1016/j.celrep.2018.03.123.

Therapeutically, fulminant diabetic mice were more efficiently treated by a vascularized islet transplant compared with the conventional approach. Given the general limitations of post-transplant vascularization associated with 3D tissue-based therapy, our approach offers a promising means of enhancing efficacy in the context of therapeutic tissue transplantation.

In Brief

Takahashi et al. report on generating vascularized islet tissue from humans and mice. After transplantation, vascularized islets significantly improve survival of diabetic mice, demonstrating the quick normalization of blood glucose compared with conventional islet transplantation.

Graphical Abstract

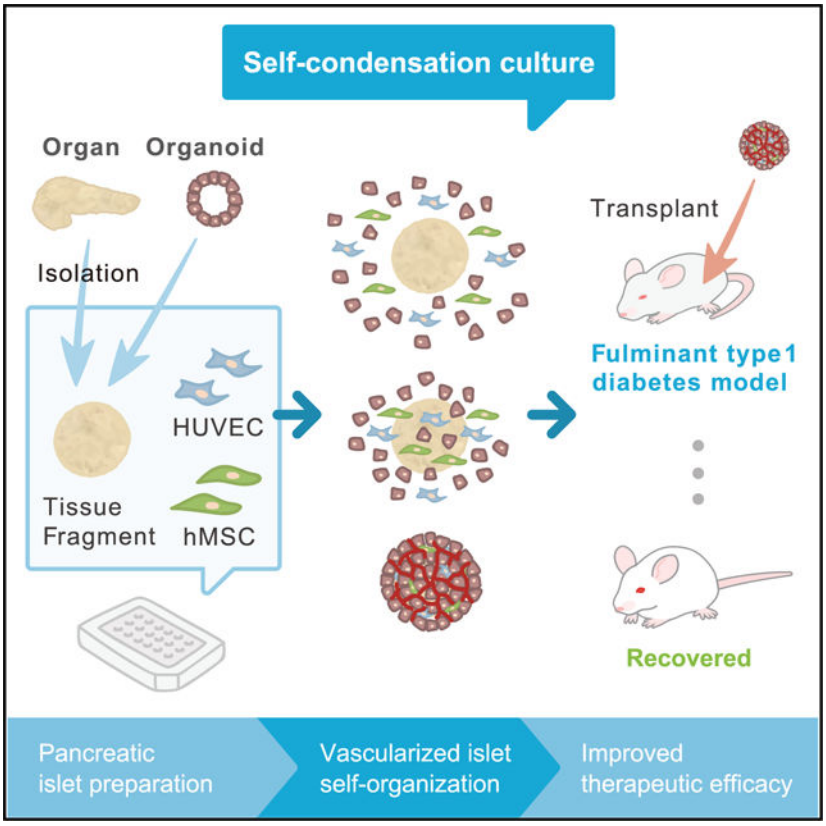

INTRODUCTION

Tissue-based therapies are gathering clinical momentum as next-generation treatments for organ dysfunction, driven by the recent success of islet transplantation. Additionally, technological innovations such as stem cell-based tissue engineering approaches highlighted tremendous therapeutic potential; however, future clinical applications of such tissue-based approaches face a critical challenge related to effective transplantation strategies that ensure efficient engraftment through the timely development of vascular networks.

A well-studied clinical example of tissue-based therapy is islet transplantation, which has successfully been used to promote insulin independence in patients with severe type 1 diabetes (Shapiro et al., 2000). However, transplanted islets have a substantially low engraftment rate because the loss of the vasculature during the isolation process induces necrosis, making it difficult to maximize the treatment efficacy of the transplant. Therefore, the rapid establishment of vascular networks is extremely important for the proper engraftment and function of transplanted islets. Recent attempts to improve post-transplant engraftment have included prevascularized niche construction (Moore et al., 2015), co-transplantation (Coppens et al., 2013; Kang et al., 2012; Oh et al., 2013), and tissue engineering (Moore et al., 2015; Perez-Basterrechea et al., 2013). Nevertheless, transplant vascularization generally takes at least 7 days, and the rapid introduction of vasculature into a transplanted tissue remains a considerable challenge.

Recently, we have developed a dynamic self-condensation approach to develop tissue organoids from dissociated organ progenitor cells in the presence of stromal vascular and mesenchymal progenitors (Takebe et al., 2014). Early success was reported using self-organizing liver buds to model early hepatogenesis, demonstrating the therapeutic potential of this strategy for treating lethal liver diseases (Takebe et al., 2013). Recent work adapting this approach to multiple organ-derived dissociated cells demonstrated the potential to generate diverse organ rudiments (organ buds) in culture (Takebe et al., 2015). Although this strategy enabled rapid blood vessel induction in tissue organoids generated from single cells in suspension, whether tissue fragments such as islet can also be adapted to follow this self-condensation principle remains unclear.

Here, we first demonstrated the adaptability of our self-condensation culture using tissue fragments from diverse organ systems, enabling endothelialized 3D tissue formation. Further studies of pancreatic islets from both humans and mice revealed that introducing an endothelial network to the culture not merely facilitates vascularization, but also improves tissue viability and functionality (insulin secretion capacity) even prior to blood perfusion. Remarkably, the resulting endothelialized islet (hereafter referred to as vascularized islet) transplants exhibited significantly improved therapeutic potential in a fulminant diabetes model through improved post-transplant engraftment. Our approach highlights the promise of using self-condensing cultures for tissue vascularization in future clinical transplantation studies.

RESULTS

Successful Self-Condensation into a 3D Vascularized Tissue from Diverse Tissue Fragments

Previously, we developed a self-condensation method for generating vascularized tissues from dissociated cell suspensions via co-culturing with human mesenchymal stem cells (MSCs) on soft substrate. Here, we adapted this approach to generate vascularized tissue from isolated adult tissue fragments or human induced pluripotent stem cell (iPSC)-derived tissues *in vitro* (Figure 1A). The results showed that applying this self-condensation approach to other tissue fragments isolated from adult animals or human pluripotent stem cell-derived tissues led to the successful formation of endothelialized and condensed tissues,

the diameter of which is applicable even up to 1,000 μm (Figure 1B; Video S1). Once human umbilical cord-derived endothelial cells (HUVECs) are included, generated tissues quickly form a functional vasculature *in vivo*.

Formation of a Vascularized Islet Using Self-Condensation Culture

We further tested the advantage of this approach by focusing on islet transplantation. First, we wanted to optimize the culture media on self-condensation culture of pancreatic islets in the presence of HUVECs and human MSCs by measuring the viability of the pancreatic islets. Mouse pancreatic islets were cultured for 3 days in RPMI 1640 medium, endothelial cell growth medium (EGM), and a combination medium (RPMI 1640 + EGM), after which a LIVE/DEAD Cell Imaging kit was used to count the number of dead cells (Figure S1A). In the islet cultures, the numbers of dead cells were 1,392 ± 485 cells/mm^2 in RPMI 1640 ($p = 0.0141$ versus RPMI 1640 + EGM; $p = 0.0095$ versus EGM), 203 ± 92.8 cells/mm^2 in RPMI 1640 + EGM ($p = 0.1152$ versus EGM), and 69 ± 70 cells/mm^2 in EGM, demonstrating that EGM is an effective culture medium for pancreatic islets (Figure S1B).

Pancreatic islets isolated from adult mice or humans were then co-cultured with fluorescently labeled HUVECs and human MSCs, and cells scattered throughout the culture well began moving toward the center to form a condensed tissue (Figures 1C, 1D, and S1C). Each condensed tissue contained pancreatic islets, with endothelial cells throughout the surrounding area (Figures 1E, S1D, and S1E). Furthermore, the measurement of insulin released into the culture medium from pancreatic islets revealed that the insulin levels in cultures containing HUVECs and human MSCs was higher than the islets alone group (Figures S1F and S1G). We then performed an *in vitro* glucose tolerance test to assess the function of the islets. In a medium containing a high concentration of glucose, the insulin levels were higher in the islets + HUVECs + human MSCs compared with the islets alone (Figure S1H). To microarray analyze, we focused on 121 endocrine lineage genes known for their role in pancreatic development, endocrine hormone secretion, and glucose metabolism (D'Amour et al., 2006; Basford et al., 2012; Bonal and Herrera, 2008). The results showed the gene expression patterns of co-cultured islets (vascularized islet) are more similar to freshly isolated islets, and cultured islets (islet alone) are totally different from freshly isolated islets (Figure 1F). These results showed that HUVECs and human MSCs released factors that enhanced the insulin secretion.

To further test the significance of endothelial and mesenchymal co-culture on islet function, we performed global gene array profiling using *in vitro* and *in vivo* transplanted vascularized islets. Microarray results showed the pancreatic gene expression signatures of transplanted vascularized islets are more similar to freshly isolated islets, but not transplanted islet alone (Figure 1F). Together, we succeeded in generating a vascularized tissue from primary islets in both mouse and human by adapting a self-condensation culture.

Improved Therapeutic Capability of Vascularized Islet Transplants

To investigate the therapeutic benefit of vascularized islet transplants in treating diabetes, we established an immunodeficient mouse model of fulminant diabetes in which hyperglycemia (>300 mg/dL) is induced via the injection of diphtheria toxin (Matsuoka et al., 2013). We

then transplanted mouse pancreatic islets under the renal capsule in the diabetic mice (Figures 2A and 2B) and examined survival rates (Figure 2C) and changes in body weight (Figure 2D) and blood glucose levels (Figure 2E). Before entering a survival experiment following fulminant diabetes, we first determined the optimal number of islets from therapeutic viewpoint alone (Figure S2). In order to examine the optimum culture and grafting conditions (the number of islets), we compared four culturing conditions on a 96-well plate: 1, 5, 10, and 20 mouse islets/well (Figure S2A). Cell viability assay showed that the number of dead cells after 24-hr culture was lowest when culture was started with one and five mouse islets per well (Figure S2B). Also, the viability of the co-cultured group (mini-sized vascularized islet) was not decreased after culture for 24 hr (Figures S2C and S2D). A steady decline in glucose levels was observed in the mice transplanted with the mini-sized vascularized mouse islet (5 islets/well × 40), but not with the mini-sized vascularized mouse islet (10 islets/well × 20) (Figure S2E), suggesting 5 islets is a well-balanced condition for efficient engraftment.

Upon this optimization, fulminant diabetic mice with or without sham transplantation were used for survival experiments. In this condition, the majority of the control mice died, and even mice transplanted with islet alone had only a 40% survival rate at post-transplantation day 5 (Figure 2C). Strikingly, more than 90% of the mice transplanted with the mini-sized vascularized islet survived ($p < 0.05$ versus islet alone). Major weight increases were observed only in the mice transplanted with the mini-sized vascularized islet, and we were able to increase their weights back to pre-hyperglycemia levels (Figure 2D). In contrast, a weight decrease, followed by sudden death (within 7 days after transplantation), was observed in the control groups of surviving mice. Steady glucose-lowering action was observed in mice transplanted with mini-sized vascularized islet or islet alone (Figure 2E). After 3 weeks, however, mice transplanted with mini-sized vascularized islet had not reverted to hyperglycemia, compared with mice transplanted with islet alone. In previous reports of co-transplantations [pancreatic islets + endothelial progenitor cells (Kang et al., 2012) and pancreatic islets + human MSC (Ito et al., 2010)], despite slight decreases, blood glucose levels were never maintained in the normal range (<200 mg/dL) for a long period of time (Figures S3A and S3B). We also performed *in vivo* glucose tolerance tests and revealed that the insulin secretory capacity of the mice transplanted with the mini-sized vascularized islet was similar to that of nondiabetic mice (Figures S3C and S3D).

Next, we transplanted mini-sized vascularized human islets under the renal capsule of immunodeficient mice (Figures S3E and S3F). Serum human insulin concentration was measured in the recipient mice. The concentrations in both the vascularized islet and islet transplant groups increased over several days following transplantation and tended to be higher in mouse in the vascularized islet transplant group at 28 days after transplantation (Figure 2F). *In vivo* glucose tolerance test showed that glucose-responsive insulin secretion tended to be higher in the vascularized islet transplant group (Figures 2G and 2H). These findings suggest that the transplantation of mini-sized vascularized islet with optimal tissue inclusion (five islets/well) significantly improves the efficacy of diabetes treatment presumably because of efficient vascularization.

The Vascularized Islet Transplants Rapidly Re-perfused *In Vivo*

To further investigate whether the vascularization is effectively promoted, we transplanted mini-sized vascularized mouse or human islets into a cranial window (CW) to track vascularization dynamics. The results showed that reperfusion of the mini-sized vascularized mouse islet started 2–3 days after transplantation (Figure 3A, upper). Similar findings were obtained in a transplant with mini-sized vascularized human islet (Figure 3B, upper), showing that the transplantation of vascularized islet induces early reperfusion. In contrast, reperfusion was observed in only 29% of mice transplanted with islets alone (Figure 3C). To discriminate between the human and mouse vasculature, we intravenously injected fluorescently labeled dextran and anti-mCD31, a specific marker of mouse endothelial cells, and performed high-resolution live imaging using confocal microscopy. We monitored the dynamics of islet engraftment and vascularization by imaging vascularized islets at days 0, 2, and 7 (Figure 3D). At day 2, we observed only a few HUVECs in the islets. At day 7, the islets showed an increased number of blood vessels formed by the HUVECs, and a rich vascular network was reconstructed around the islets, with blood circulating inside the vessels (Figures 3D–3F; Video S2). At post-transplantation day 7, each islet exhibited a blood vessel area of approximately 11.5% ± 4.0% (islet transplantation [Tx]) and 45.0% ± 17.2% (vascularized islet) ($p = 0.0022$ for vascularized islet Tx versus islet Tx), the latter of which was comparable with the proportion observed in the adult mouse islets (Figure 3J). Similarly, in vascularized human islet, reperfusion was observed inside the human blood vessels formed by the HUVECs (Figures 3H–3J). We also transplanted islets that had been vascularized by fluorescently labeled HUVECs and human MSCs, which revealed that the human blood vessels formed by HUVECs had connected with the host mouse vessels, with blood circulating inside the vessels (Figure 3K). Moreover, the human MSCs were located adjacent to the human blood vessels (Figure 3L). These findings demonstrate the formation process of stable human vascular networks within mice. First, vascular endothelial cells migrate, proliferate, and form premature tubes, thereby establishing leaky blood vessels. Then, they underwent extensive remodeling and stabilized by an MSC to become non-leaky mature vessels. In fact, our intravital imaging showed blood vessels were still immature 3 days after transplantation, whereas at 7 days tissues become mature enough to reconstruct the non-leaky functional vascular network after transplantation (Figure 3F). Interestingly, the islets themselves did not exhibit reperfusion or morphological changes in mice transplanted with islet alone, and the number of live islets decreased over time (Figures 3A and 3B, lower). In addition, almost no blood circulation was observed inside the islets (Figure 3G). The above findings suggest the potential rationale for improved efficacy because the transplantation of vascularized islet induces early reperfusion and enhances engraftment.

The Proportion of Cells in Transplanted Vascularized Islets Was Similar to that in Pancreatic Islets

Because matrix proteins in the basement membrane are known to be essential for the proliferation and survival of pancreatic β cells, we further performed a histological evaluation of matrix protein expression in the transplanted grafts (Figures 4A and 4B). H&E staining revealed pancreatic islet engraftment in both groups without central necrosis. Immunostaining of transplanted vascularized islet revealed the presence of human endothelial cells in the insulin-positive area, as well as the production of laminin ($p < 0.0001$

for vascularized islet versus islet alone) and collagen IV ($p = 0.2$ for vascularized islet versus islet alone) (Figures 4C and 4D). In contrast, almost no laminin or collagen IV was expressed in the transplanted islet alone. Immunostaining for endocrine cells (pancreatic α, β, and δ cells) to evaluate the structure of the transplanted islets showed endocrine cell-positive areas of approximately 52,719 ± 25,396 μm^2 (vascularized islet) and 21,818 ± 15,113 μm^2 (islet alone) (Figures 4E and 4F). Comparing the cell composition inside the transplanted islets revealed that the proportions of α, β, and δ cells were approximately 91.4% ± 1.8% ($p = 0.1920$ versus pancreatic islet; $p = 0.0008$ versus islet Tx), 7.4% ± 1.6% ($p = 0.2416$ versus pancreatic islet; $p = 0.0006$ versus islet Tx), and 1.3% ± 0.86% ($p = 0.8926$ versus pancreatic islet; $p = 0.5949$ versus islet Tx), respectively, for vascularized islet and 94.6% ± 2.3% ($p = 0.0114$ versus pancreatic islet), 4.2% ± 2.4% ($p = 0.0055$ versus pancreatic islet), and 1.2% ± 0.52% ($p = 0.6406$ versus pancreatic islet) for islet alone (Figures 4G–4I). These results indicated that the proportion of cells in the transplanted vascularized islet was similar to that of endogenous pancreatic islets. In particular, the proportion of α cells in the vascularized islet was approximately 1.8 times greater than that in the islet alone. It is unlikely that increase in the proliferation rate was selective to pancreatic α cells in the presence of both HUVECs and human MSCs, suggesting that the results were due to increase in the viability of pancreatic α cells. Furthermore, ultrastructural analyses of the transplanted islet using electron microscopy showed that the characteristic core-mantle structure of the pancreatic islet (β cells at the center and α and δ cells in the periphery) was maintained only in the vascularized islet (Figures 4J–4L). Together, these findings suggest that the transplantation of vascularized islet not merely contained a stable human vasculature with basement membrane, but exhibited the normal physiological functional structure due to a maintained endocrine component among various islet cells such as α and β cells, possibly contributing to an observed favorable outcome in the diabetic model.

DISCUSSION

Tissue engineering potentially provides a promising therapeutic paradigm toward organ replacement, but has yet to be applied in humans partly because of the lack of effective transplant strategy. The timely coordination of tissue vascularization within engineered tissue is necessary to ensure survival and functionality *in vitro* and tissue engraftment *in vivo*. Here, using multiple types of cells with tissue fragments, we successfully integrated 3D tissue structures with vascular networks by adapting self-condensation culture. The major advancements over previous self-condensation methods include the increased scale of the tissue fragments for integrating supportive lineages such as endothelial lineages. Second, the effective use of primary tissues for pancreatic application outweighs the use of MIN6 cells for future clinical application (Takebe et al., 2015), because MIN6 cells were isolated from an insulinoma of a transgenic (Tg) mouse expressing the SV40 T antigen in pancreatic islet β cells. Third, given that recently evolving organoid-based approaches mostly lack vasculatures, our methodology described here will serve as a complementary approach to build additional complexity into engineered tissues or organoids. Thus, a self-condensation approach not only shows promise for regenerative medicine, but can also serve as novel

platforms for disease modeling and drug discovery by reconstructing more complex and heterotypic structure.

The present study clearly showed that pancreatic islets isolated from adult mice and humans were capable of establishing vascular networks *in vitro* when co-cultured with HUVECs and human MSCs under appropriate conditions. The close relationship between pancreatic islets and endothelial cells is known to be extremely important for islet function. Pancreatic islets secrete vascular endothelial growth factor (VEGF)-A to activate endothelial cells, thereby facilitating vascularization. In addition to their involvement in blood flow within pancreatic islets, endothelial cells are known to associate with many factors, including an angiocrine factor that modulates the proliferation and function of pancreatic β cells (hepatocyte growth factor [HGF]) and connective tissue growth factor (CTGF), as well as extracellular matrix proteins. For example, our *in vitro* experiment showed that co-culture with HUVECs and human MSCs increased the expression levels of various cytokines (e.g., CTGF) (data not shown), suggesting that these growth factors effectively enhance survival and insulin secretion in pancreatic islets. Human MSCs also produce angiogenic growth factors (VEGF-A, interleukin [IL]-6, IL-8, HGF, and PDGF) to enhance vascularization and basement membrane formation in islets. Laminin, which is produced as the basement membrane, was previously shown to bind to integrin receptors expressed on the surface of pancreatic β cells, thereby enhancing proliferation and insulin production. In addition, collagen IV is produced by endothelial cells and interacts with α1β1-integrin to enhance insulin secretion (Eberhard et al., 2010), which in turn promotes vascularization and basement membrane production, thereby inducing insulin production and pancreatic β cell proliferation. Our morphological observations of the vascularized islet grafts confirmed the distribution of endothelial cells within endocrine tissues, along with the abundant expression of laminin and collagen IV. Therefore, the transplantation of vascularized islet appears to establish a beneficial local environment around the islets, wherein cellular interactions occur to enhance the survival and function of transplanted pancreatic islets through various mechanisms (e.g., the production of angiogenesis factors and basement membrane), potentiating islet homeostasis and function.

The immediate challenges of islet transplantation are to treat patients with a minimal number of donors and to achieve stable and long-term glycemic control after transplantation. Our approach enabled drastic improvements in the survival rates in fulminant diabetic mice followed by multiple mechanism of action analyses, including islet engraftment rates, insulin secretion function, and glucose responsiveness, highlighting the possibility of halting long-term insulin therapy through the clinical use of vascularized islet. In other words, our approach may help decrease the number of donors required to treat a single patient and may serve as a principal curative strategy in treating type 1 diabetes, of which there are 79,000 new diagnoses per year worldwide.

Current limitation of this approach involves the use of two distinct stromal progenitors especially about HUVEC. Endothelial cells that are transplanted from a donor into a genetically unrelated recipient will be possibly rejected by the recipient’s immune system. One possible way to minimize this problem is through the use of immunocompatible or autologous pluripotent stem cells for generation of endothelial lineages (Kane et al., 2011;

Giuliani et al., 2011; Takebe et al., 2017). However, several issues must still be addressed before pluripotent stem cell-derived cells can be used in the clinic. For example, the risk of teratomas and other types of tumors caused by the residual immature cells cannot be completely eliminated. Emerging studies with the use of encapsulation devices will alleviate this concern (Kirk et al., 2014). Additionally, Shapiro and colleagues demonstrated a potential ectopic (subcutaneous) site by developing vascularized pockets in mice (Pepper et al., 2015). This technique reportedly overcame the physical and physiological problems associated with transplantation, thereby opening up a safer approach for imaging, biopsy, local immune modulation, and stem cell therapy. Together, a combination of our vascularization strategy shown in the present study with the findings of regenerative studies using pluripotent stem cells and the transplantation technology reported by others will be thus likely to provide an alternative transplantation approach for patients who respond poorly to conventional islet transplantation.

EXPERIMENTAL PROCEDURES

Retroviral Transduction

For live imaging, the cells were infected with retroviruses expressing GFP or KOFP as previously described (Takebe et al., 2012). In brief, the retroviral vector pGCDNsam IRESEGFP or KOFP was used to transfect 293GP and 293GPG packaging cells (provided by Masafumi Onodera, National Research Institute for Child Health and Development, Tokyo, Japan), in which viral particle production was triggered using a tetracycline-inducible system (Suzuki et al., 2002). The supernatants were collected from the retrovirus-infected cultures, passed through a 0.45-μm filter (Whatman; GE Healthcare), and immediately used for infection. KOFP displays a major absorption maximum at 548 nm, with a slight shoulder at 515 nm, and bright orange fluorescence, with an emission peak at 561 nm.

Mouse Islets

Pancreatic islets were isolated from 8- to 12-week-old male C57BL/6 (Japan SLC) or Tg (CAG-GFP) mice (Okabe et al., 1997; Li et al., 2009). The mice were bred and maintained according to the institutional guidelines for the use of laboratory animals of Yokohama City University (approval no. F-A-17–026). After the abdomens of mice anesthetized with diethyl ether (Wako) were disinfected with 70% ethanol, laparotomy was performed, and it was noted that the ligated ampulla of Vater is a binding part of the common bile duct and duodenum. Then, Hank's balanced salt solution (HBSS; GIBCO) and collagenase XI (1,000 U/mL) (Cat. No. C7657; Sigma) were inserted by using a 27G needle in the merging portion of cystic duct and hepatic duct. The excised pancreas was placed in a 50-mL tube containing collagenase XI solution and was shaken for 15 min at 37.5°C. After the pancreas was digested, ice-cold HBSS (including 1 mM $CaCl_2$) was added. After cleaning with 25 mL of solution and centrifugation (290 × *g*, 30 s, 4°C), the supernatant was removed. Again, the sample was cleaned, and after centrifugation, it was added to 15 mL of HBSS and filtered using a cell strainer of 70 μm mesh residue, and placed in their own prepared medium for the culture of islets. The isolated islets were hand-picked using a pipette, counted, and placed in a 5% CO_2 incubator at 37°C.

Human Islets

Human islet preparations from deceased donors were processed for clinical transplantation at the University of Alberta and were made available for research when the islet yield fell below that of the minimal mass required for clinical transplantation, and consent was obtained from next of kin (Kin et al., 2011). Permission for use of human islets was granted by the Health Research Ethics Board of the University of Alberta. Human islets from 53 donors were used in this study.

Tissue Fragments

After anesthetized 8- to 12-week-old male C57BL/6 mice with diethyl ether were disinfected with 70% ethanol, we performed cardiac transluminal perfusion. The brain, heart, small intestine, kidney, liver, and lung were excised, washed with physiological saline, and minced with scissors on ice. There were collected and filtered by using a cell strainer of 100 μm mesh. It was filtered using a cell strainer of 70 μm mesh to flow through, and finally filtered through a cell strainer of 40 μm mesh to flow through. The remaining cell mass (cell strainer 40 μm mesh) were collected using EGM.

Induced Pluripotent Stem Cell Tissues

Human iPSCs were seeded in each well of a six-well plate at a density of 1.0×10^6 cells per well. Cells were cultured in a 37°C incubator to prepare a sphere of 50–500 μm in diameter. The iPSC spheres were hand-picked using a pipette and counted.

Culture

The isolated islets were cultured in EGM (CC-4133; Lonza) containing 10% fetal bovine serum (Biowest), 20 mM L-glutamine (GIBCO), 100 U/mL penicillin (GIBCO), and 100 μg/mL streptomycin (GIBCO) at 37°C in a humidified 5% CO_2 incubator. HUVECs and human MSCs (Lonza) were maintained in EGM (Lonza) or MSC growth medium (Lonza) at 37°C in a humidified 5% CO_2 incubator. To generate vascularized islets or tissue fragments or iPSC tissues *in vitro*, each well of a 48-well plate was coated with 150 μL of Matrigel (BD Biosciences) diluted in an equal volume of medium, followed by a 10-min incubation at 37°C. The islets or tissue fragments or iPSC tissues, ~1×10^5 HUVECs and ~2×10^4 human MSCs, were then suspended in medium and plated in each well on the presolidified Matrigel. 3D tissues formed autonomously after approximately 24 hr of culture.

Miniaturization of Vascularized Islet

Isolated islets were aggregated in culture medium using low-cell-adhesion 96-well plates with U-bottomed conical wells (Sumitomo Bakelite). ~5 islets, ~5×10^3 HUVECs, and ~1×10^3 human MSCs were suspended in medium and plated in each well. Vascularized islets formed autonomously after approximately 24 hr of culture and were transplanted into the left subrenal area of the mouse.

In Vitro Insulin Secretion

100 islets were plated into 24-well transwell membrane inserts (BD Biosciences). 2×10^4 HUVECs and 4×10^3 human MSCs were cultured in lower transwell chambers. The

experiment was divided into two groups as follows: islets (control), and islets + HUVEC and human MSC. After 24 hr, insulin levels in the culture media were measured using a mouse insulin ELISA kit (Shibayagi) or Insulin Human ELISA Kit Mercodia (Funakoshi) according to the manufacturer's instructions.

In Vitro Glucose Stimulated Insulin Secretion

100 mouse islets were plated into 48-well transwell membrane inserts (BD Biosciences). 1×10^4 HUVECs and 2×10^3 human MSCs were cultured in lower transwell chambers. The experiment was divided into two groups as follows: islets (control), and islets + HUVEC and human MSC. A glucose challenge test was performed using 60 mg/dL (1 hr) and 360 mg/dL (1 hr) glucose dissolved in RPMI 1640 medium (Wako) for simulating low- and high-glucose conditions, respectively. Insulin levels in the cell culture media were measured using a mouse insulin ELISA kit.

Graft Function

Mice (8- to 12-week-old male severe combined immunodeficiency [SCID] Ins-TRECK-Tg) (Matsuoka et al., 2013) weighing approximately 20 g each were intraperitoneally (i.p.) injected with 1 μg/kg body weight of diphtheria toxin to induce diabetes (blood glucose levels over 300 mg/dL) for 3 days. SCID Ins-TRECK-Tg mice were expressing the diphtheria toxin receptor under control of the human *INS* and mouse *ins2* promoters by the toxin receptor-mediated cell knockout method (Saito et al., 2001). After 3 days of consistent hyperglycemia, animals were transplanted with islets. The body weights and blood glucose levels of the diabetic mice were monitored daily. Islets that were co-cultured for 24 hr served as the experimental group, and an equal amount (200 islets) of islet-only cultures served as the control. After 1 month, the transplanted tissues were removed from the animals.

Human islets (400 islets) were transplanted into the left subrenal area of the non-obese diabetic (NOD)/SCID mouse (Sankyo Lab.) (8- to 12-week-old male). After every 7 days, human insulin levels in the recipient were measured using an insulin Ultrasensitive ELISA Kit (Funakoshi) according to the manufacturer's instructions.

Microarray Analysis

Total RNA was prepared from mouse adult islets, primary islet, cultured islet (day 1), and transplanted islet (day 7) using an RNeasy Mini Kit (Life Technologies). RNA for gene-expression profiling was hybridized on a SurePrint G3 Mouse GE microarray 8×60K Ver. 2.0 (Agilent Technologies) according to the manufacturer's instructions. To microarray analyze, we focused on 121 endocrine lineage genes known for their role in pancreatic development, endocrine hormone secretion, and glucose metabolism (D'Amour et al., 2006; Basford et al., 2012; Bonal and Herrera, 2008).

Glucose Tolerance Test

The mice were fasted for 16 hr and then intraperitoneally injected with 3 g/kg body weight of glucose. Serum human insulin concentrations were measured using an Insulin Human ELISA Kit Mercodia according to the manufacturer's instructions. The area under the curve was calculated using standard methods.

Intravital Imaging

For intravital imaging, vascularized islets were transplanted into a pre-formed cranial window in a NOD/SCID mouse (Takahashi et al., 2014; Takebe et al., 2012). The transplantation procedures were described in our previous work (Takebe et al., 2014). The *in vivo* fate of the transplanted cells was monitored by intravital imaging using a Leica TCS SP5 confocal microscope (Leica Microsystems). Tail-vein injections of 1% tetramethylrhodamine-conjugated dextran (molecular weight [MW] 2×10^6) or fluorescein-isothiocyanate-conjugated dextran (MW 2×10^6) were used to identify the vessel lumens (all from Invitrogen). An Alexa Fluor 647-conjugated mouse-specific CD31 antibody (BD) was intravenously injected into the mice to visualize the murine vasculature (Takebe et al., 2014). Confocal image stacks were acquired for the implanted vessels and dextran. Image projections were processed using MetaMorph Angiogenesis Module software (Molecular Devices). The percentage of vessel area per islet area was then automatically logged into an Excel spreadsheet.

Tissue Processing and Immunostaining

The tissues were fixed overnight in 4% paraformaldehyde at 4°C, processed, and embedded in paraffin. Transverse sections (5 μm) were placed on microscope slide adhesive (MAS)-coated slides (Matsunami Glass) for immunostaining or standard histological staining with H&E. Immunostaining was preceded by autoclave antigen retrieval in citrate buffer (pH 6.0). The primary antibodies were anti-insulin, anti-human CD31, anti-laminin (all from Dako Corporation), anti-glucagon (Sigma), anti-somatostatin, anti-desmin, and anti-collagen IV (all from Merck Millipore). The tissue sections were incubated with an Alexa Fluor-conjugated secondary antibody (Life Technologies) for 1 hr at room temperature, followed by DAPI (Sigma) nuclear staining. The images were acquired on an LSM510 laser scanning microscope (Carl Zeiss).

Electron Microscopy

The samples were fixed with 2% paraformaldehyde and 2% glutaraldehyde in 0.1 M phosphate buffer at 4°C. The further sample preparation and images were captured by Tokai Electron Microscopy.

Statistics

The data are expressed as the mean ± SD of at least three independent experiments. The number of experiments is shown in the figure legends.

Supplementary Material

Refer to Web version on PubMed Central for supplementary material.

ACKNOWLEDGMENTS

We thank Asuka Kodaka for illustration materials. We also appreciate N. Hijikata, M. Enomura, K. Takeuchi, and the members of our laboratory for support. This work was primarily supported by grants from PRESTO and the Japan Science and Technology Agency (JST) to T.T. and partly by Grants-in-Aid from the Ministry of Education, Culture, Sports, Science and Technology of Japan to T.T. (grants 24106510 and 24689052) and H.T. (grants 21249071 and 25253079). This work was also partly supported by the AMED through its research grant “Research

Center Network for Realization of Regenerative Medicine" and a grant from the Japan IDDM network to H.T. This project was supported in part by PHS Grant P30 DK078392 (Pathology core) of the Digestive Disease Research Core Center in CCHMC and Just-in-Time Core Grant Program in CCTST to T.T. T.T. is a New York Stem Cell Foundation Robertson Investigator.

REFERENCES

Basford CL, Prentice KJ, Hardy AB, Sarangi F, Micallef SJ, Li X, Guo Q, Elefanty AG, Stanley EG, Keller G, et al. (2012). The functional and molecular characterisation of human embryonic stem cell-derived insulin-positive cells compared with adult pancreatic beta cells. Diabetologia 55, 358–371. [PubMed: 22075915]

Bonal C, and Herrera PL (2008). Genes controlling pancreas ontogeny. Int. J. Dev. Biol. 52, 823–835. [PubMed: 18956314]

Coppens V, Heremans Y, Leuckx G, Suenens K, Jacobs-Tulleneers-Thevissen D, Verdonck K, Lahoutte T, Luttun A, Heimberg H, and De Leu N. (2013). Human blood outgrowth endothelial cells improve islet survival and function when co-transplanted in a mouse model of diabetes. Diabetologia 56, 382–390. [PubMed: 23090187]

D'Amour KA, Bang AG, Eliazer S, Kelly OG, Agulnick AD, Smart NG, Moorman MA, Kroon E, Carpenter MK, and Baetge EE (2006). Production of pancreatic hormone-expressing endocrine cells from human embryonic stem cells. Nat. Biotechnol. 24, 1392–1401. [PubMed: 17053790]

Eberhard D, Kragl M, and Lammert E. (2010). 'Giving and taking': endothelial and b-cells in the islets of Langerhans. Trends Endocrinol. Metab. 21, 457–463. [PubMed: 20359908]

Giuliani M, Oudrhiri N, Noman ZM, Vernochet A, Chouaib S, Azzarone B, Durrbach A, and Bennaceur-Griscelli A. (2011). Human mesenchymal stem cells derived from induced pluripotent stem cells down-regulate NK-cell cytolytic machinery. Blood 118, 3254–3262. [PubMed: 21803852]

Ito T, Itakura S, Todorov I, Rawson J, Asari S, Shintaku J, Nair I, Ferreri K, Kandeel F, and Mullen Y. (2010). Mesenchymal stem cell and islet co-transplantation promotes graft revascularization and function. Transplantation 89, 1438–1445. [PubMed: 20568673]

Kane NM, Xiao Q, Baker AH, Luo Z, Xu Q, and Emanueli C. (2011). Pluripotent stem cell differentiation into vascular cells: a novel technology with promises for vascular re(generation). Pharmacol. Ther. 129, 29–49. [PubMed: 20965210]

Kang S, Park HS, Jo A, Hong SH, Lee HN, Lee YY, Park JS, Jung HS, Chung SS, and Park KS (2012). Endothelial progenitor cell cotransplantation enhances islet engraftment by rapid revascularization. Diabetes 61, 866–876. [PubMed: 22362173]

Kin T, O'Gorman D, Schroeder A, Onderka C, Richer B, Rosichuk S, Zhai X, and Shapiro A. (2011). Human islet distribution program for basic research at a single center. Transplantation Proc. 43, 3195–3197.

Kirk K, Hao E, Lahmy R, and Itkin-Ansari P. (2014). Human embryonic stem cell derived islet progenitors mature inside an encapsulation device without evidence of increased biomass or cell escape. Stem Cell Res. (Amst.) 12, 807–814.

Li D-S, Yuan Y-H, Tu H-J, Liang QL, and Dai LJ (2009). A protocol for islet isolation from mouse pancreas. Nat. Protoc. 4, 1649–1652. [PubMed: 19876025]

Matsuoka K, Saito M, Shibata K, Sekine M, Shitara H, Taya C, Zhang X, Takahashi TA, Kohno K, Kikkawa Y, and Yonekawa H. (2013). Generation of mouse models for type 1 diabetes by selective depletion of pancreatic beta cells using toxin receptor-mediated cell knockout. Biochem. Biophys. Res. Commun. 436, 400–405. [PubMed: 23747725]

Moore SJ, Gala-Lopez BL, Pepper AR, Pawlick RL, and Shapiro AJ (2015). Bioengineered stem cells as an alternative for islet cell transplantation. World J. Transplant. 5, 1–10. [PubMed: 25815266]

Oh BJ, Oh SH, Jin SM, Suh S, Bae JC, Park CG, Lee MS, Lee MK, Kim JH, and Kim KW (2013). Co-transplantation of bone marrow-derived endothelial progenitor cells improves revascularization and organization in islet grafts. Am. J. Transplant. 13, 1429–1440. [PubMed: 23601171]

Okabe M, Ikawa M, Kominami K, Nakanishi T, and Nishimune Y. (1997). 'Green mice' as a source of ubiquitous green cells. FEBS Lett. 407, 313–319. [PubMed: 9175875]

Pepper AR, Gala-Lopez B, Pawlick R, Merani S, Kin T, and Shapiro AM (2015). A prevascularized subcutaneous device-less site for islet and cellular transplantation. Nat. Biotechnol. 33, 518–523. [PubMed: 25893782]

Perez-Basterrechea M, Obaya AJ, Meana A, Otero J, and Esteban MM (2013). Cooperation by fibroblasts and bone marrow-mesenchymal stem cells to improve pancreatic rat-to-mouse islet xenotransplantation. PLoS ONE 8, e73526. [PubMed: 24009755]

Saito M, Iwawaki T, Taya C, Yonekawa H, Noda M, Inui Y, Mekada E, Kimata Y, Tsuru A, and Kohno K. (2001). Diphtheria toxin receptor-mediated conditional and targeted cell ablation in transgenic mice. Nat. Biotechnol. 19, 746–750. [PubMed: 11479567]

Shapiro AM, Lakey JR, Ryan EA, Korbutt GS, Toth E, Warnock GL, Kneteman NM, and Rajotte RV (2000). Islet transplantation in seven patients with type 1 diabetes mellitus using a glucocorticoid-free immunosuppressive regimen. N. Engl. J. Med. 343, 230–238. [PubMed: 10911004]

Suzuki A, Obi K, Urabe T, Hayakawa H, Yamada M, Kaneko S, Onodera M, Mizuno Y, and Mochizuki H. (2002). Feasibility of ex vivo gene therapy for neurological disorders using the new retroviral vector GCDNsap packaged in the vesicular stomatitis virus G protein. J. Neurochem. 82, 953–960. [PubMed: 12358801]

Takahashi Y, Takebe T, Enomura M, Koike N, Lee S, Nemeno J, Sekine K, Lee J, and Taniguchi H. (2014).). High-resolution intravital imaging for monitoring the transplanted islets in mice. Transplantation Proc. 43, 1166–1168.

Takebe T, Koike N, Sekine K, Enomura M, Chiba Y, Ueno Y, Zheng Y-W, and Taniguchi H. (2012). Generation of functional human vascular network. Transplantation Proc. 44, 1130–1133.

Takebe T, Sekine K, Enomura M, Koike H, Kimura M, Ogaeri T, Zhang R-R, Ueno Y, Zheng Y-W, Koike N, et al. (2013). Vascularized and functional human liver from an iPSC-derived organ bud transplant. Nature 499, 481–484. [PubMed: 23823721]

Takebe T, Zhang R-R, Koike H, Kimura M, Yoshizawa E, Enomura M, Koike N, Sekine K, and Taniguchi H. (2014). Generation of a vascularized and functional human liver from an iPSC-derived organ bud transplant. Nat. Protoc. 9, 396–409. [PubMed: 24457331]

Takebe T, Enomura M, Yoshizawa E, Kimura M, Koike H, Ueno Y, Matsuzaki T, Yamazaki T, Toyohara T, Osafune K, et al. (2015). Vascularized and complex organ buds from diverse tissues via mesenchymal cell-driven condensation. Cell Stem Cell 16, 556–565. [PubMed: 25891906]

Takebe T, Sekine K, Kimura M, Yoshizawa E, Ayano S, Koido M, Funayama S, Nakanishi N, Hisai T, Kobayashi T, et al. (2017). Massive and reproducible production of liver buds entirely from human pluripotent stem cells. Cell Rep 21, 2661–2670. [PubMed: 29212014]

Highlights

- Self-condensation culture enables endothelialization of diverse tissue fragments
- Vascularization facilitates tissue survival after transplantation
- Vascularized islet transplant enhances therapeutic potential against diabetes
- Rapid induction of functional vasculatures preserves original islet architecture

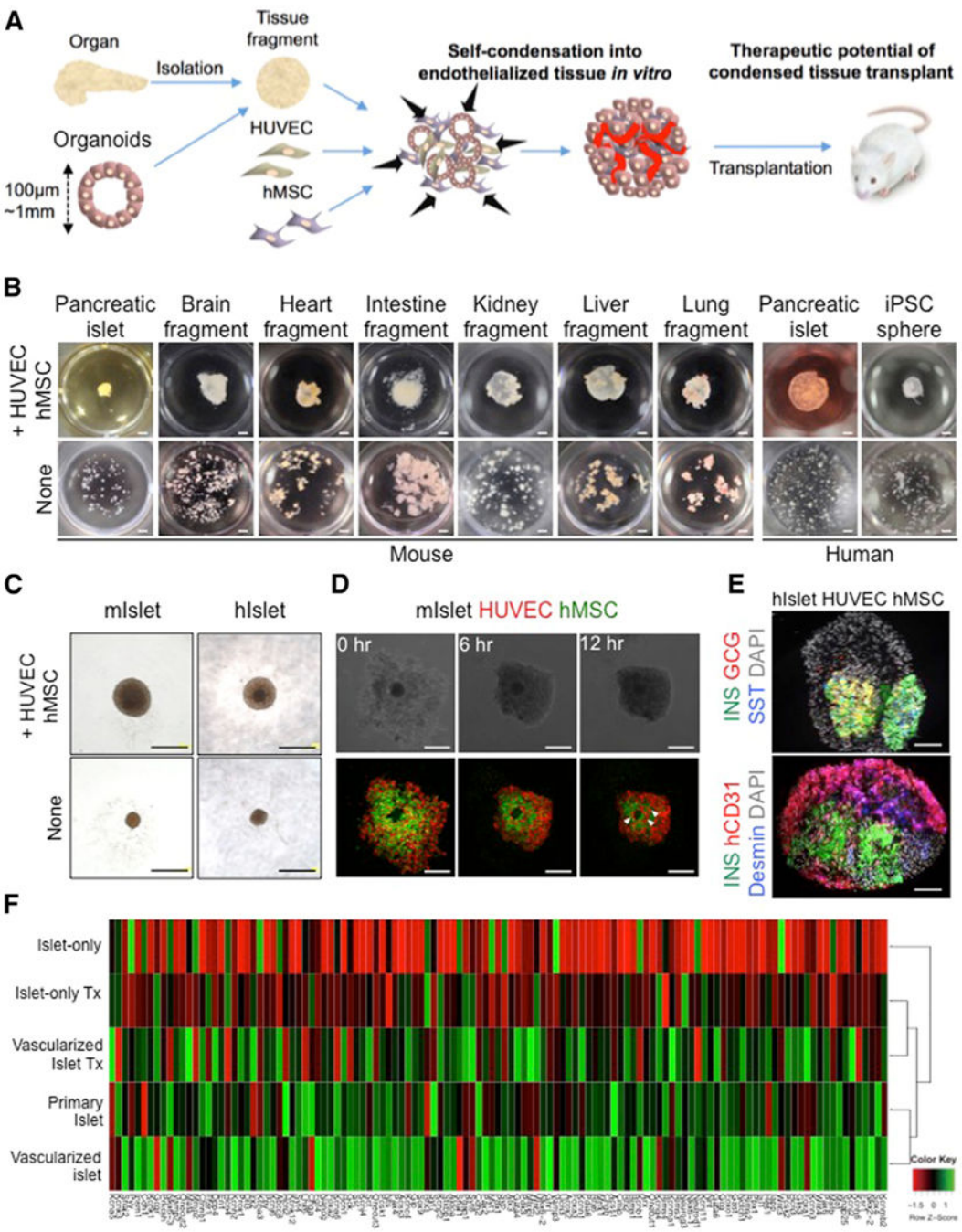

Figure 1. Self-Condensation into Endothelialized Tissues from Diverse Tissue Fragments

(A) General strategy for creating endothelialized tissue fragments *in vitro*.

(B) The endothelialization technique is adaptable to all tissue types examined in this study, including islets, brain fragments, heart fragments, intestine fragments, kidney fragments, liver fragments, lung fragments, and even spheroids of induced pluripotent stem cells. Scale bars, 1,000 μm.

(C) Gross observation of a mini-sized vascularized islet (upper) and an islet alone (lower). Scale bars, 500 μm.

(D) Formation of a three-dimensional mini-sized vascularized mouse islet in co-cultures of islets with HUVECs and human MSCs. The arrowheads indicate the blood vessel-like structures. Scale bars, 250 μm.

(E) Immunofluorescence staining of the pre-transplantation vascularized islet (upper) and islet alone (lower). GCG, glucagon; hCD31, human CD31; INS, insulin; SST, somatostatin. Scale bars, 100 μm.

(F) Hierarchical clustering of the pancreatic lineage 121 genes with the relevance in pancreatic development or β cell function. Each row in the heatmap represents a sample, and each column represents the expression level of a gene. The color scale below the heatmap represents the raw *Z* score ranging from green (high expression) to red (low expression).

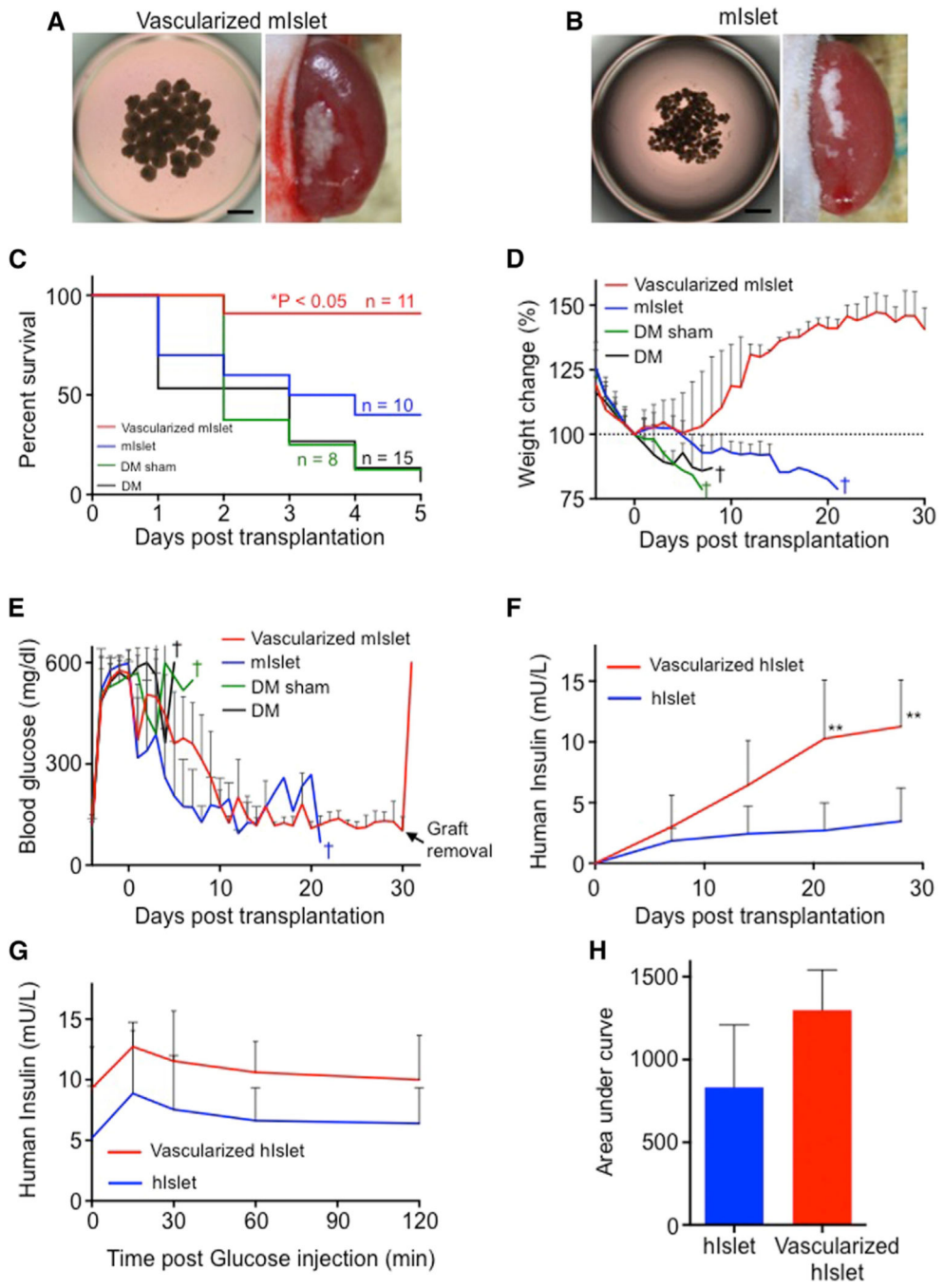

Figure 2. Vascularized Islet Self-Condensation Enables Efficient Therapeutic Transplantation

(A and B) Brightfield image of the collected vascularized mouse islet (A), islet alone (B), and recipient kidneys after transplantation. Scale bars, 500 μm.

(C) Kaplan-Meier survival curves of the diabetic mice. *p < 0.05.

(D) Percentage of body weight variations in the diabetic mice. The data represent the mean ± SD. n = 11 vascularized mouse islet, n = 10 mouse islet alone, n = 8 diabetes mellitus (DM) sham mice, and n = 15 DM mice.

(E) Blood glucose measurements of the progressively diabetic mice. The glucose measurements were saturated at 600 mg/dL. The data represent the mean ± SD. n = 11 vascularized mouse islet, n = 10 islet alone, n = 8 DM sham mice, and n = 15 DM mice.
(F) *In vivo* human insulin secretion. The data represent the mean ± SD. n = 5 vascularized human islet and n = 8 human islet alone. **p < 0.01; *p < 0.05.
(G) Glucose tolerance testing 35 days after transplantation. The data represent the mean ± SD. n = 4 vascularized human islet and n = 4 human islet alone.
(H) Area under the curve for (G). The data represent the mean ± SD. n = 4 vascularized human islet and n = 4 human islet alone.

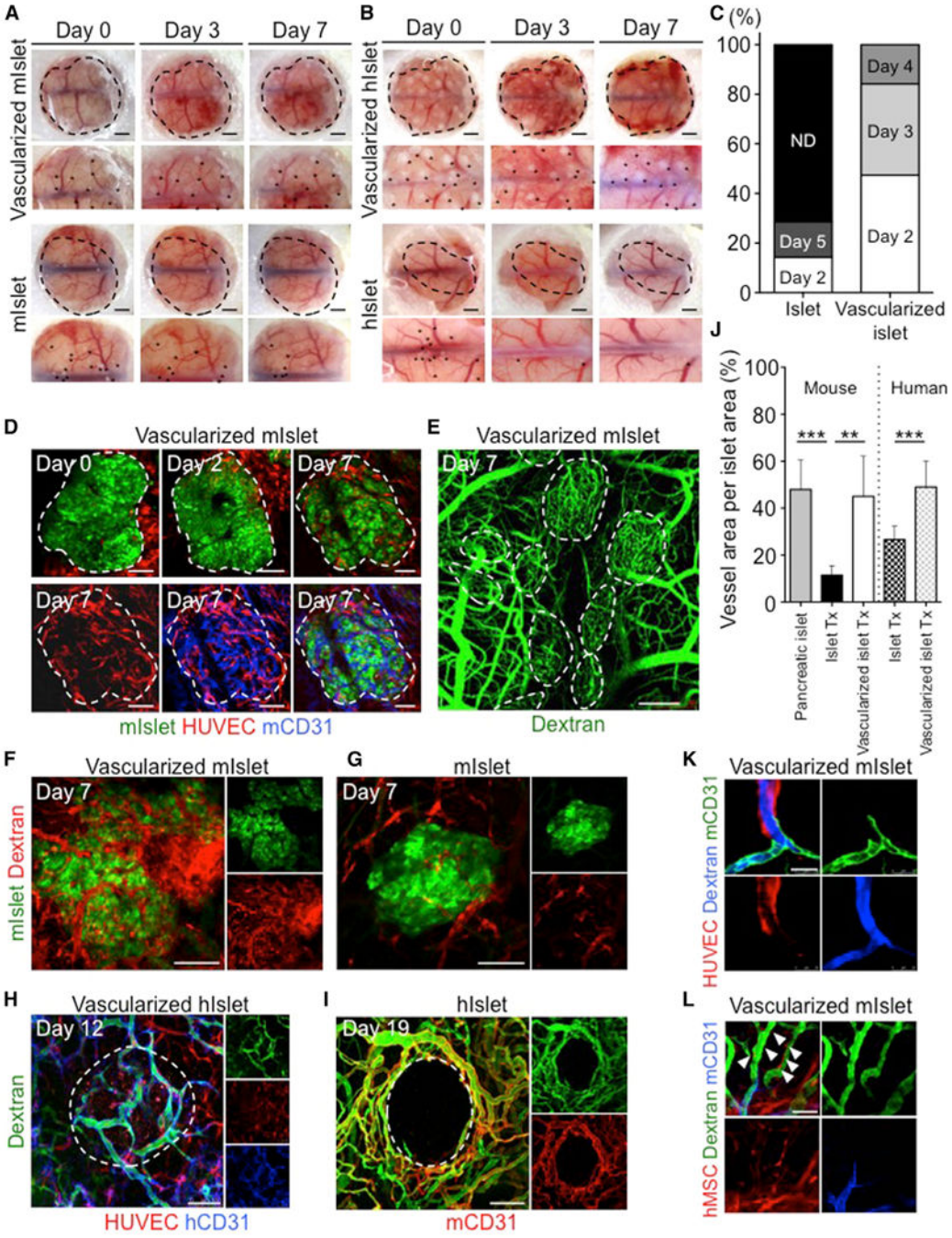

Figure 3. Rapid Induction of Functional Vascular Networks *In Vivo*

(A–C) Macroscopic observation of the transplanted mini-sized vascularized islet (n = 19) (A) and islet alone (n = 7) (B) at multiple time points, showing the rapid perfusion of blood vessels (C). Asterisk indicates the transplants. Scale bars, 1,000 μm. ND, not detected.

(D) Intravital tracking of a vascularized mouse islet. Islet, green; HUVECs, red; human MSCs, unlabeled; mouse CD31, blue. The dotted area indicates the transplants. Scale bars, 100 μm.

(E) Dextran infusion showing recipient circulation. The dotted area indicates the mouse islet. Scale bar, 250 μm.

(F and G) Intravital imaging of a vascularized mouse islet (F) and mouse islet alone (G) 7 days after transplantation. Islet, green; HUVECs and human MSCs, unlabeled; dextran, red. Scale bars, 100 μm.

(H and I) Intravital imaging of a vascularized human islet (H) and a human islet alone (I) after transplantation. Islet, unlabeled; HUVECs, red; human MSCs, unlabeled; dextran, green; human CD31, blue; mouse CD31, red. The dotted area indicates the islet. Scale bars, 100 μm.

(J) Quantification of the dextran-positive area. The data represent the mean ± SD. ***$p < 0.001$; **$p < 0.01$ ($n = 3, 5, 6, 8$, and 5 mouse pancreatic islet, mouse islet alone Tx, vascularized mouse islet Tx, human islet alone, and vascularized human islet, respectively).

(K) Visualization of the connections between HUVECs and host vessels at day 14. Mouse CD31, green; HUVECs, red; dextran, blue. Scale bar, 25 μm.

(L) Localization of human MSCs at day 14. Arrowheads indicate hMSC localization in perivascular region.

Dextran, green; human MSC, red; mouse CD31, blue. Scale bar, 50 μm.

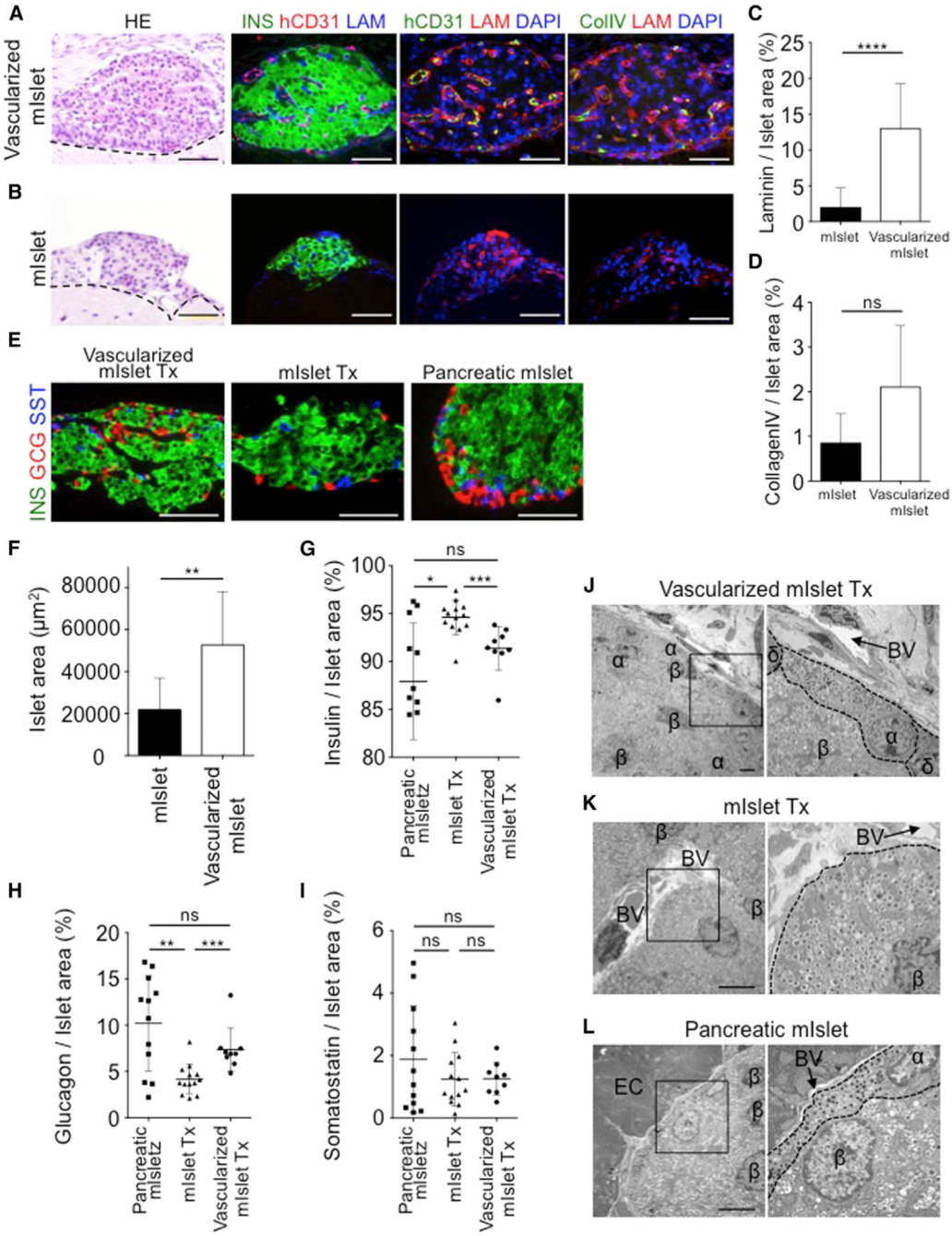

Figure 4. Preservation of Natural Islet Components in the Vascularized Islet Transplant

(A and B) H&E and immunofluorescence staining of the grafts from a vascularized mouse islet Tx (A) and mouse islet alone Tx (B) at day 35. The dotted line indicates the border on the brain. Col IV, collagen IV; hCD31, human CD31; INS, insulin; LAM, laminin. Scale bars, 50 μm.

(C and D) Quantification of the laminin-positive (n = 29) (C), and collagen IV-positive (n = 3) (D) areas. Data represent the mean ± SD. ****p < 0.0001. ns, not significant.

(E) Immunofluorescence staining of the grafts at day 35. GCG, glucagon; INS, insulin; SST, somatostatin. Scale bars, 50 μm.

(F) Quantification of the endocrine cells in the graft. Mouse islet alone, n = 10; vascularized mouse islet, n = 9. **p < 0.01.

(G–I) Quantification of the insulin-positive (G), glucagon-positive (H), and somatostatin-positive (I) areas in the graft. The data represent the mean ± SD. n = 12 mouse pancreatic islet Tx, n = 13 mouse islet alone, and n = 9 vascularized mouse islet Tx. ***p < 0.001; **p < 0.01; *p < 0.05. ns, not significant.

(J–L) Electron microscopy of the vascularized mouse islet Tx (J), mouse islet Tx (K), and pancreatic mouse islet (L) at 35 days. α, alpha cell; β, beta cell; δ, delta cell; BV, blood vessel; EC, exocrine cell. Scale bars, 5 μm